Proc. Natl. Acad. Sci. USA
Vol. 86, pp. 8635–8639, November 1989
Biochemistry

Structure of a bacterial enzyme regulated by phosphorylation, isocitrate dehydrogenase

(x-ray crystallography/protein structure/NADP$^+$ binding/lactate dehydrogenase fold/protein phosphorylation)

JAMES H. HURLEY*, PETER E. THORSNESS†‡, V. RAMALINGAM*, NANCY H. HELMERS*, DANIEL E. KOSHLAND, JR.†, AND ROBERT M. STROUD*

*Department of Biochemistry and Biophysics and Graduate Group in Biophysics, University of California, San Francisco, CA 94143-0448; and †Department of Biochemistry, University of California, Berkeley, CA 94720

Contributed by Daniel E. Koshland, Jr., July 31, 1989

ABSTRACT **The structure of isocitrate dehydrogenase [*threo*-D_S-isocitrate:NADP$^+$ oxidoreductase (decarboxylating), EC 1.1.1.42] from *Escherichia coli* has been solved and refined at 2.5 Å resolution and is topologically different from that of any other dehydrogenase. This enzyme, a dimer of identical 416-residue subunits, is inactivated by phosphorylation at Ser-113, which lies at the edge of an interdomain pocket that also contains many residues conserved between isocitrate dehydrogenase and isopropylmalate dehydrogenase. Isocitrate dehydrogenase contains an unusual clasp-like domain in which both polypeptide chains in the dimer interlock. Based on the structure of isocitrate dehydrogenase and conservation with isopropylmalate dehydrogenase, we suggest that the active site lies in an interdomain pocket close to the phosphorylation site.**

The isocitrate dehydrogenase (IDH) of *Escherichia coli* [*threo*-D_S-isocitrate:NADP$^+$ oxidoreductase (decarboxylating), E.C. 1.1.1.42] is subject to a unique mechanism of regulatory control. This enzyme lies at a key branch point in carbohydrate metabolism, which is extremely sensitive to regulation (1–5); it is converted from an active to a completely inactive form upon phosphorylation (1).

The reaction catalyzed by IDH is a step in the citric acid cycle, and is shown below:

$$\text{NADP}^+ + \text{isocitrate} \rightarrow \text{NADPH} + \alpha\text{-ketoglutarate} + CO_2$$

The enzyme was shown to be phosphorylated (6, 7) and the phosphorylation was shown to occur on a serine residue (8). Although there is some loss of activity when Ser-113 is replaced by a number of amino acids (Ala, Cys, Thr, Tyr), the replacement by aspartic acid causes complete inactivation (9). Hence, it is the negative charge introduced by phosphorylation that causes inactivation (9).

There is no significant sequence conservation between IDH and any of the dehydrogenases for which three-dimensional structures are known. The sequence of *E. coli* IDH shows significant conservation only with isopropylmalate dehydrogenase (IMDH) (9). A preliminary x-ray diffraction pattern has been reported for IMDH (10). Aligned residues of IDH and IMDH sequences (11–14) are 25–29% identical, varying among species.

The structures of dehydrogenases have been the subject of much interest because the nucleotide-binding domains of many of these enzymes retain much structural similarity, despite relatively little sequence conservation, as first observed by Rossman *et al.* (15). This nucleotide-binding fold is referred to as the lactate dehydrogenase (LDH) fold, for the first enzyme in which it was described (16). The same fold has been described, with small modifications, in many other structures, frequently in a nucleotide-binding domain. As IDH shows no sequence conservation with dehydrogenases of known structure, the IDH structure is of interest as a potential alternative solution to the same evolutionary challenge.§

Structure Determination

IDH was purified by a modification of the procedure described by Reeves *et al.* (17) from a strain of *E. coli* in which IDH was expressed as described by LaPorte *et al.* (18). Crystals were grown in a solution containing dephosphorylated IDH (28 mg/ml), 34% saturated ammonium sulfate, 100 mM NaCl, 35 mM Na_2HPO_4, 9 mM citric acid, and 0.2 mM dithiothreitol at pH 5.4. Crystals grew to a size of 0.8 mm along the largest dimension after 2 weeks. Unit cell parameters are $a = b = 105.1$ Å, $c = 150.3$ Å, and the space group is $P4_32_12$. The asymmetric unit is the monomer; two monomers are related by crystallographic twofold symmetry.

Diffraction was observed to 2.5 Å with Cu Kα radiation from a rotating anode x-ray source at room temperature. All diffraction data were collected on a Nicolet area detector and reduced with the XENGEN data reduction package. One isomorphous heavy atom derivative was prepared by a 5-day soak in 1% saturated *p*-chloromercuribenzenesulfonic acid (PCMBS). The position of one major site was determined from the heavy-atom difference Patterson map, with a second site subsequently located from an error residual map. Heavy atom parameters were refined by the method of Dickerson *et al.* (19) and a single isomorphous replacement electron density map was calculated. Crystallographic statistics as a function of resolution are summarized in Fig. 1.

Density modification (20) resulted in a dramatic improvement of the electron density map. The unusually large solvent fraction of 0.73 facilitated the use of density modification in phasing. The phases calculated by a first round of density modification were fixed and used for further refinement of heavy atom parameters; a second single isomorphous replacement map was used in a new round of density modification, and a second density-modified phase set was calculated. Ten cycles of density modification resulted in a final *R* factor of 28% and a mean figure of merit of 0.76.

The main chain was built into a 2.8-Å electron density map as polyalanine with FRODO (21). Phase combination between a 375-residue partial structure and single isomorphous replacement phases allowed us to fit amino acid sequence to the

The publication costs of this article were defrayed in part by page charge payment. This article must therefore be hereby marked "*advertisement*" in accordance with 18 U.S.C. §1734 solely to indicate this fact.

Abbreviations: IDH, isocitrate dehydrogenase; IMDH, isopropylmalate dehydrogenase; LDH, lactate dehydrogenase; PCMBS, *p*-chloromercuribenzene sulfonic acid.

‡Present address: Section of Genetics and Development, Cornell University, Ithaca, NY 14853.

§The atomic coordinates described here have been deposited in the Protein Data Bank at Brookhaven (accession no. 1IDH).

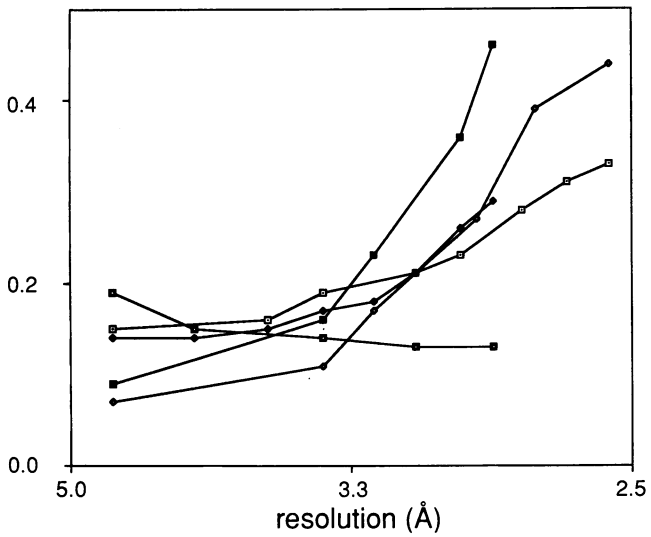

FIG. 1. Crystallographic statistics. □, $R_c = \Sigma|F_o - F_c|/\Sigma F_o$, summed over 17,948 reflections with $|F|/\sigma(F) > 3$; F_o and F_c are the observed and calculated amplitudes. ◇, Native R_{merge}; ■, PCMBS derivative R_{merge}. $R_{merge} = \Sigma|I_i - \langle I\rangle|/\Sigma\langle I\rangle$, summed over all observations from all crystals. Of 30,209 reflections possible from 25–2.5 Å, 27,951 were measured for native, and of 21,668 reflections possible from 25–2.8 Å, 20,055 were measured for the PCMBS derivative. The average redundancy of measurement was 4.25 for the native data set and 3.0 for the derivative; the overall unweighted merging R factor on intensity was 0.12 for five native crystals and 0.14 for three derivative crystals. ◆, $\langle\Delta F\rangle/\langle F\rangle = \Sigma_w|F_{ph} - F_p|/\Sigma_w F_p$, where $w = 1/\sigma^2$, and σ is the estimated error. Weighting is used so that $\langle\Delta F\rangle/\langle F\rangle$ approximates the true difference in amplitudes, rather than the increase of R merge with resolution. The mean unweighted absolute value of $\Delta F/F$ between native and derivative data sets is 0.21. □, $0.1 \times \langle FH\rangle/\varepsilon$ is the mean absolute value of the PCMBS heavy atom structure factor divided by the estimated rms lack of closure error, based on centric reflections only. $R_{Cullis} = 0.58$ for the PCMBS derivative; $R_{Cullis} = \Sigma^{\|}F_{ph} \pm F_p| - F_h|/\Sigma|F_{ph} \pm F_p|$, where the summation is over all centric reflections. PCMBS statistics are shown for heavy atom parameters refined with phases calculated by a first round of density modification.

electron density for the entire model. PCMBS sites are at Cys-332 and Cys-405. Refinement then proceeded with alternate cycles of minimization using PROLSQ (22) and XPLOR (23) and manual rebuilding with the aid of $(2F_o - F_c)\alpha_{calc}$ Fourier syntheses. The placement of some 40 residues changed substantially during refinement; 7 residues were added in the N-terminal region. The $(2F_o - F_c)\alpha_{calc}$ maps based on phases calculated after refinement with PROLSQ after removal of residues in question were used to test the model; these led to no reconnections. The current model has been refined by simulated annealing using XPLOR for 1 ps at 2000 K and 0.25 ps at 300 K, followed by minimization and manual rebuilding into a 2.5-Å map. The first four residues from the N terminus have not been placed in electron density in the current model. The fit of side chains to electron density (Fig. 2) is generally excellent, and carbonyl oxygens can be seen in almost all of the map. The crystallographic R factor is currently 19.7% for 17,948 reflections with $|F|/\sigma(F) > 3$ from 5.0 to 2.5 Å (Fig. 1). The rms deviations of bond lengths and angles from ideal values are 0.017 Å and 3.4°, respectively.

The Structure of IDH

Domain Structure. IDH consists of three domains: a large $\alpha + \beta$ domain, a small α/β domain, and an α/β clasp-like domain involving both subunits (Figs. 3 and 4). The large and small domains are built around a common 12-stranded β-

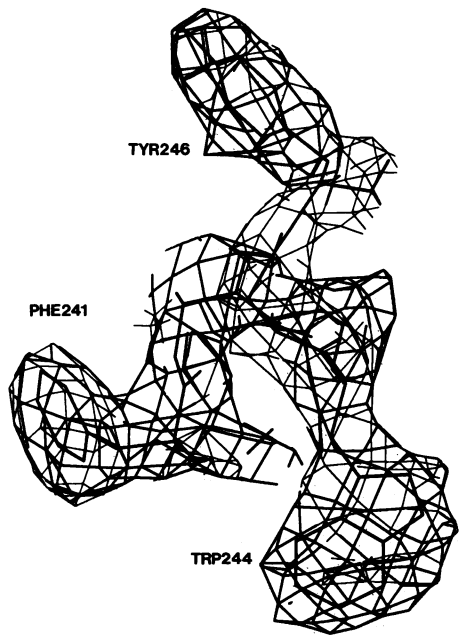

FIG. 2. Electron density from a 2.8 Å $(2F_o - F_c)\alpha_{calc}$ map for residues 241–246 . The three aromatic side chains in the sequence Phe-Lys-Asp-Trp-Gly-Tyr made this a distinctive marker for assignment of known sequence to the model. Lys and Asp side chains are not visible in this view.

sheet. A very distinct cleft separates the large and small domains, and except for the sheet they are folded indepen-

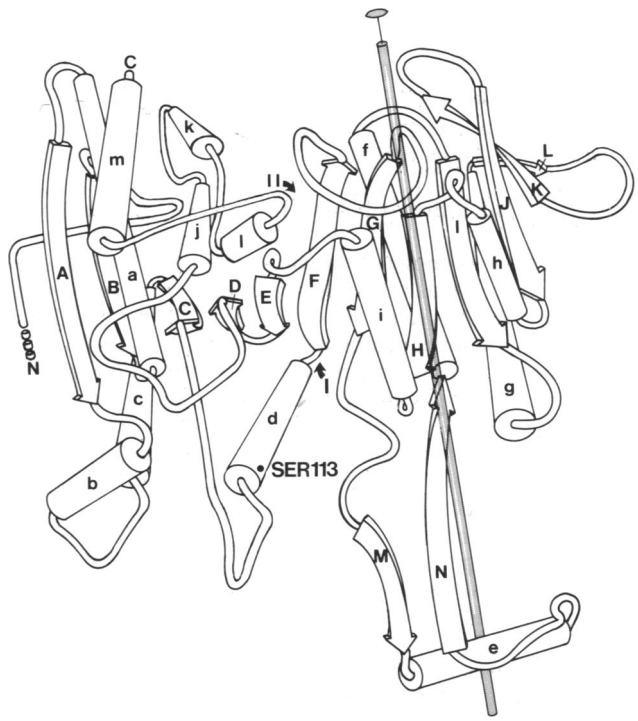

FIG. 3. Diagram of the IDH monomer. The large $\alpha+\beta$ domain containing the N and C termini is to the left, the small α/β domain is to the right, and the clasp-like domain is pointing down. The domains are separated between strands E and F. Helices are labeled in alphabetical order as they occur in the chain, and strands are labeled as they occur in the two β-sheets, from left to right in this view. Roman numerals I and II designate the front and rear pockets. The shaded rod represents the crystallographic twofold axis of symmetry that relates the two subunits.

FIG. 4. Carbon α trace of IDH. The phosphorylation site at Ser-113, the C terminus at Met-416, the first well-ordered residue in the model, Val-5, and other residues of interest are labeled in this divergent stereo view.

dently, each with its own hydrophobic core. Two pockets line the cleft between the large and small domains, one on either side of the sheet. We refer to the pockets formed in front of and behind the sheet (as viewed in Fig. 3) as the "front" and "rear" pockets. The exceptionally large β-sheet is mixed parallel and antiparallel and comprises 270° of a turn of superhelix, which has the normal left-handed sense; 99% of the expected sequence has been located; IDH is 46% helical, 22% sheet, 19% coil, and 12% turn.

The small domain consists of residues 125–157 and 203–317 and is a typical α/β sandwich structure. The large domain consists of residues 1–124 and 318–416. This domain has a helical subdomain consisting of helices a, j, k, l, and m, and a large α/β subdomain, which makes up the rest of the large domain. Helices a and j are packed against the sheet, hence belonging to both the helical bundle and the α/β subdomains.

The clasp-like domain is formed by the interlocking about the crystallographic twofold axis of the polypeptide segments consisting of residues 158–202 from both subunits (Fig. 5). A flat four-stranded antiparallel β-sheet is formed by two strands from each subunit. A hydrophobic core is formed only in the dimer by the packing of the helices against each other and the sheet. The small domain as well as the clasp-like domain are involved in intersubunit contacts. Helices h and i form extensive hydrophobic contacts with helices i′ and h′ (where the ′ denotes the other subunit). Residues 140 and 234–236, which are in loops and at the start of the g helix, are also involved in intersubunit contacts.

Phosphorylation Site. The phosphorylation site at Ser-113 is on helix d at the edge of the front pocket (Fig. 6). Most of the regions of highest conservation between IDH and IMDH sequences (Fig. 7) are in the cleft. Strands D, F, and G, part of the floor of both pockets, are all at least 50% conserved. Also highly conserved are helix i and loops 230–234 and 339–347, in the front pocket region, and helix j. Strand N (Fig. 7) is not present in IMDH, and strand M is not conserved. Three conserved arginines, Arg-119, -129, and -153, near Ser-113, and His-339, the only conserved histidine, are in the front pocket. Lys-230′, another conserved residue, also points into this pocket. The rear pocket is highly hydrophobic, and includes residues Tyr-125, Leu-128, Ile-328, Phe-335, and Met-362, similar or identical in IMDH.

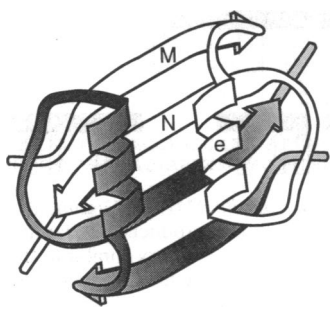

FIG. 5. Diagram of the clasp-like domain, shown looking down the crystallographic twofold axis. One subunit is shaded.

Discussion

Topology. The topology of IDH (Fig. 8) is quite distinct from that described for the known dehydrogenase structures. Best known is the lactate dehydrogenase-like class, including LDH (16), malate dehydrogenase (25), alcohol dehydrogenase (26), glyceraldehyde-3-phosphate dehydrogenase (27), and L-3-hydroxyacyl CoA dehydrogenase (28). Although the catalytic domains vary in structure, the nucleotide-binding domains of these enzymes all have a very similar structure, the LDH fold, and all bind the cofactor in a similar manner. The LDH fold consists of a $\beta\alpha\beta\alpha\beta$ motif, with the β-strands arranged in parallel and linked by parallel helices. In the LDH-like dehydrogenases, the motif is repeated twice and is also referred to as a "dinucleotide-binding fold"; a single $\beta\alpha\beta\alpha\beta$ unit is also referred to as a "mononucleotide-binding fold." Minor variations, such as the absence of a single helix, occur within this family. Many other proteins, either nucleotide-binding or with other functions, are topologically similar to the LDH-like class; an extensive review of α/β topologies is given by Richardson (29). Only $NAD(P)^+$-binding proteins are discussed here.

A second group of dehydrogenases has structural similarity to glutathione reductase (30) and includes trimethylamine dehydrogenase (31) and lipoamide dehydrogenase (32). These enzymes have only an LDH-like mononucleotide-binding fold within a larger parallel sheet. Still less similar to LDH, dihydrofolate reductase (33) contains an LDH-like mononucleotide-binding fold within a mixed parallel and antiparallel sheet.

Nearly all known α/β nucleotide-binding domains exploit the partial positive charges at the N termini of parallel α-helices in binding the negatively charged phosphate moities of the nucleotide (34). Among the dehydrogenases, so far only 6-phosphogluconate dehydrogenase (35), an α-helical protein, is outside the α/β class. Beef liver catalase binds NADPH near the C terminus of a helix (36), although the function of NADPH in this system is unknown. The IDH structure contains four α-helices in a parallel arrangement packed on either side of a section of parallel β-sheet, in a manner typical of nucleotide-binding domains. Although the location of bound $NADP^+$ has yet to be determined, it is possible that the IDH fold has evolved to provide the same electrostatic enhancement of nucleotide binding by terminal partial charges of parallel helices enjoyed by the LDH-like enzyme class.

Although the topology of IDH is quite distinct from that of LDH, part of the small domain of IDH consists of parallel helices packed on either side of a parallel section of β-sheet, resembling the LDH-like mononucleotide-binding domain. This feature contains the four parallel strands G–J and helices f–i. If the clasp-like domain and strands K and L were removed, the arrangement in the sheet of strands G–J num-

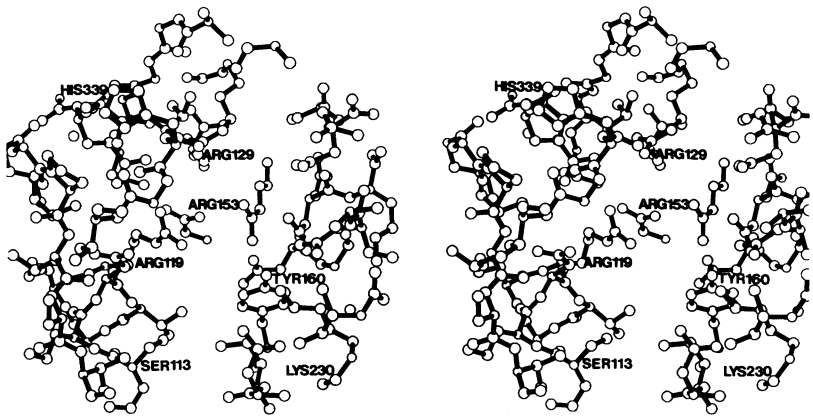

FIG. 6. Divergent stereo view of the front interdomain pocket of IDH. Side chains are shown for selected conserved residues and Ser-113. Both subunits are shown; Lys-230 belongs to the second subunit.

bered as they occur in the sequence would be 1, 4, 2, 3. If the connections to strands G and H were exchanged, the arrangement in the sheet would then be 4, 1, 2, 3. Helices f and g would then connect strands 1, 2, and 3, forming an LDH-like mononucleotide-binding fold. Careful inspection of an electron density map calculated with phases from a model refined after omitting strands G and H assures us, however, that these connections cannot be exchanged.

To compare the IDH and LDH structures in three dimensions, helices f and g and strands G–J of IDH, and helices B and C and strands D, A, B, and C of LDH[¶] were superposed by least squares. The rms deviation between the main chain atoms of these 50 residues is only 2.8 Å. The rest of the 152 residues in the small domain of IDH do not superpose well with the LDH nucleotide-binding domain. Only a few types of supersecondary structure are common in proteins, and secondary structural elements in α/β structures tend to pack at the same angles in diverse proteins (37). Topologies of IDH and LDH are dissimilar, and evolutionary relatedness cannot be inferred solely from similar supersecondary structure.

[¶]Main chain atoms of residues 208–221, 239–251, 149–154, 297–302, 223–228, and 275–279 of IDH and residues 31–44, 53–65, 92–97, 23–28, 48–53, and 77–81 of pig heart LDH were included in the superposition.

IDH contains a fold that has not previously been described. Within the spectrum of topologies of α/β structures in NAD(P)$^+$-binding proteins, the small domain of IDH is among the most different from the LDH fold. We expect the overall structure of IMDH to be similar, although probably lacking a separate clasp-like domain and without the N-terminal loop of IDH. It is likely that the evolutionary histories of IDH and related enzymes are different from those of most other dehydrogenases.

Clasp-like Domain. The unusual interlocking clasp-like domain is based on a β-sheet in which both identical polypeptide chains from the dimer contribute strands. The 60° packing angle of helices with the sheet and the hydrogen-bonding of symmetry-related strands make this domain similar to that formed jointly by the α_1 and α_2 domains in the class I human leukocyte antigen (38). Among other examples, the subunit interface in alcohol dehydrogenase (27) contains two sets of symmetry-related antiparallel β-strands.

Conservation, Binding, Catalysis, and Regulation. The phosphorylation site at Ser-113 (Fig. 6) is sufficiently close to the subunit interface to allow direct interactions between the phosphoserine and the other subunit. In contrast to the case of glycogen phosphorylase, in which the region of the phosphorylation site is well ordered only in the phosphoenzyme (39), Ser-113 and surrounding residues of dephosphorylated

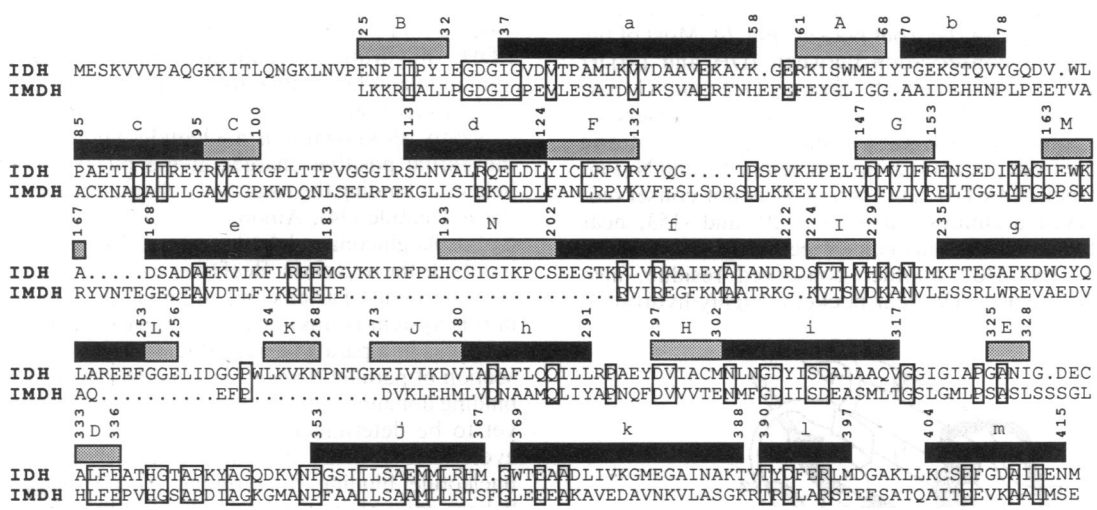

FIG. 7. Alignment of amino acid sequences (single-letter code) of *E. coli* IDH and *Bacillus subtilis* IMDH. Alignments of IDH to IMDH sequences from *Thermus aquaticus* (11), *B. subtilis* (12), *Bacillus caldotenax* (13), and *Candida utilis* (14) produced similar identities. Two other available sequences, from *Thermus thermophilus* and *Saccharomyces cerevisiae* were not used, as they are very similar to the *T. aquaticus* and *C. utilis* sequences. Pairwise sequence alignments using a standard algorithm (24) of IDH and IMDH sequences were modified by hand to eliminate gaps in conserved regions of secondary structure where possible. Residues that are identical in *E. coli* IDH and *B. subtilis* IMDH sequences are boxed. Secondary structures of IDH are shown above the corresponding sequence; β-strands and α-helices are designated by shaded and solid bars above the sequence and are labeled with capital and lowercase letters, respectively. Numbering is for the IDH sequence; numbers are included for end points of regular secondary structures.

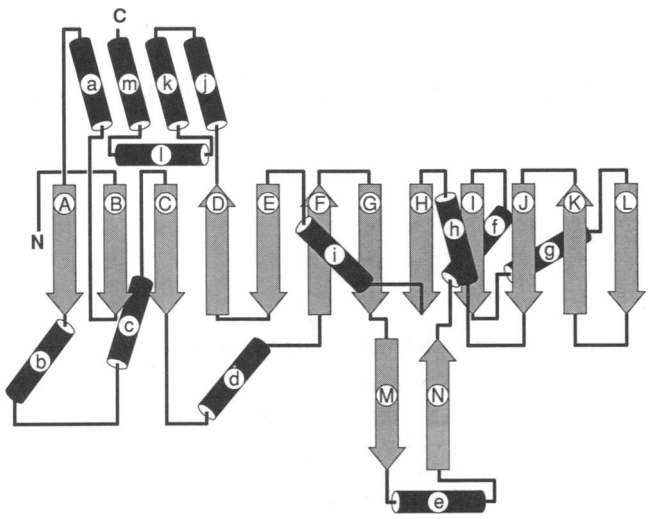

FIG. 8. Schematic diagram of the IDH fold. A table of other protein topologies is found in ref. 29.

IDH are well ordered. Ser-113 is on the protein surface, presumably accessible to IDH kinase/phosphatase. Ser-113 is also at the edge of the front pocket, compatible with a possible direct phosphoserine-substrate interaction. There is a cluster of conserved residues in the pocket, including Arg-119, Arg-129, Arg-153, Tyr-160, and Lys-230′. The conserved positive charges suggest a binding site for negatively charged substrates and perhaps a means for stabilizing the oxyanion intermediate that is believed to occur in the IDH reaction. Lys-230′ is in the loop 230–234 adjoining the pocket, suggesting that both subunits participate in each active site. The only conserved histidine, His-339, is also in this pocket, in the highly conserved loop 339–347, and is a candidate for the acid–base catalyst normally present in dehydrogenases. The exceptional hydrophobicity and the high level of conservation in the rear pocket suggest some functional importance for this pocket as well.

As demonstrated in glycogen phosphorylase, regulatory covalent modifications and allosteric control can cause conformational changes that propagate over large distances (39). Covalent phosphorylation of IDH is particularly dramatic because the negative charge on the phosphoserine reduces activity to essentially zero. Whether the regulatory effect is through a conformational change, a direct change effect on one or more of the substrates, or a combination of the two awaits the structural analysis of the phosphoenzyme and complexes with substrate and cofactor.

We thank Janet Finer-Moore and William Montfort for valuable comments on the structural analysis, J. Fernando Bazan for suggestions concerning sequence comparisons, and Tony Dean for helpful discussions. Eric Fauman assisted in preliminary characterization of IDH crystals, and Julie Newdoll helped prepare Figs. 3 and 5. This work was supported by National Institutes of Health Grant GM 24485 to R.M.S. and National Science Foundation Grant 04200 to D.E.K. Crystallographic refinement was carried out in part on Pittsburgh Supercomputer Center facilities under Grant DMB890040P. J.H.H. thanks the University of California Regents for a fellowship.

1. LaPorte, D. C. & Koshland, D. E., Jr. (1983) *Nature (London)* **305,** 286–290.
2. Kornberg, H. L. & Madsen, N. B. (1951) *Biochim. Biophys. Acta* **24,** 651–653.
3. Kornberg, H. L. (1966) *Biochem. J.* **99,** 1–11.
4. Holms, W. H. & Bennett, P. M. (1971) *J. Gen. Microbiol.* **65,** 57–68.
5. LaPorte, D. C., Walsh, K. & Koshland, D. E., Jr. (1984) *J. Biol. Chem.* **259,** 14068–14075.
6. Garnak, M. & Reeves, H. C. (1979) *J. Biol. Chem.* **254,** 7915–7920.
7. Wang, J. Y. J. & Koshland, D. E., Jr. (1982) *Arch. Biochem. Biophys.* **218,** 59–67.
8. Borthwick, A. C., Holms, W. H. & Nimmo, H. G. (1984) *Biochem. J.* **222,** 797–804.
9. Thorsness, P. E. & Koshland, D. E., Jr. (1987) *J. Biol. Chem.* **262,** 10422–10425.
10. Katsube, Y., Tanaka, N., Takenaka, A., Yamada, T. & Oshima, T. (1988) *J. Biochem.* **104,** 679–680.
11. Kagawa, Y., Nojima, H., Nukiwa, N., Ishizuka, M., Nakajima, T., Yasuhara, T., Tanaka, T. & Oshima, T. (1984) *J. Biol. Chem.* **259,** 2956–2960.
12. Imai, R., Sekiguchi, T., Nosoh, Y. & Tsuda, K. (1987) *Nucleic Acids Res.* **15,** 4988.
13. Sekiguchi, T., Suda, M., Ishii, T., Nosoh, Y. & Tsuda, K. (1987) *Nucleic Acids Res.* **15,** 853.
14. Hamasawa, K., Kobayashi, Y., Harada, S., Yoda, K., Yamasaki, M. & Tamura, G. (1987) *J. Gen. Microbiol.* **133,** 1089–1097.
15. Rossman, M. G., Moras, D. & Olsen, K. W. (1974) *Nature (London)* **250,** 194–199.
16. Adams, M. J., Ford, G. C., Koekok, R., Lentz, P. J., Jr., McPherson, A., Jr., Rossmann, M. G., Smiley, I. E., Schevitz, R. W. & Wonacott, A. J. (1970) *Nature (London)* **227,** 1098–1103.
17. Reeves, H. C., Gaston, O. D., Chen, C. L. & Houston, M. (1972) *Biochim. Biophys. Acta* **258,** 27–39.
18. LaPorte, D. C., Thorsness, P. E. & Koshland, D. E., Jr. (1985) *J. Biol. Chem.* **260,** 10563–10568.
19. Dickerson, R. E., Weinzierl, J. E. & Palmer, R. A. (1968) *Acta Crystallogr. Sect. B* **24,** 997–1003.
20. Wang, B. C. (1985) *Methods Enzymol.* **115,** 90–111.
21. Jones, T. A. (1985) *Methods Enzymol.* **115,** 157–170.
22. Hendrickson, W. A. (1985) *Methods Enzymol.* **115,** 252–270.
23. Brunger, A. T., Kuriyan, K. & Karplus, M. (1987) *Science* **235,** 458–460.
24. Devereux, J., Haeberli, P. & Smithies, O. (1984) *Nucleic Acids Res.* **12,** 387–395.
25. Hill, E., Tsernoglou, D., Webb, L. & Banaszak, L. J. (1972) *J. Mol. Biol.* **72,** 577–591.
26. Branden, C. I., Eklund, H., Nordstrom, B., Boiwe, T., Soderlund, G., Zeppezauer, E., Ohlsson, I. & Akeson, A. (1973) *Proc. Natl. Acad. Sci. USA* **70,** 2439–2442.
27. Buehner, M., Ford, G. C., Moras, D., Olsen, K. W. & Rossmann, M. G. (1973) *Proc. Natl. Acad. Sci. USA* **70,** 3052–3054.
28. Birktoft, J. J., Holden, H. M., Hamlin, R., Xuong, N. H. & Banaszak, L. J. (1987) *Proc. Natl. Acad. Sci. USA* **84,** 8262–8266.
29. Richardson, J. S. (1981) *Adv. Protein Chem.* **34,** 167–339.
30. Thieme, R., Pai, E. F., Schirmer, R. H. & Schulz, G. E. (1981) *J. Mol. Biol.* **152,** 763–782.
31. Lim, L. W., Shamala, N., Mathews, F. S., Steenkamp, D. J., Hamlin, R. & Xuong, N. (1986) *J. Biol. Chem.* **261,** 15140–15146.
32. Takenaka, A., Kizawa, K., Hata, T., Sato, S., Misaka, E., Tamura, C. & Sasada, Y. (1988) *J. Biochem.* **103,** 463–469.
33. Wierenga, R. K., De Maeyer, M. C. H. & Hol, W. G. J. (1985) *Biochemistry* **24,** 1346–1357.
34. Adams, M. J., Archibald, I. G., Bugg, C. E., Carne, A., Gover, S., Helliwell, J. R., Pickersgill, R. W. & White, S. W. (1983) *EMBO J.* **2,** 1009–1014.
35. Matthews, D. A., Alden, R. A., Bolin, J. T., Filman, D. J., Freer, S. T., Hamlin, R., Hol, W. G. J., Kisliuk, R. L., Pastore, E. J., Plante, L. T., Xuong, N. & Kraut, J. (1978) *J. Biol. Chem.* **253,** 6946–6954.
36. Fita, I. & Rossman, M. G. (1985) *Proc. Natl. Acad. Sci. USA* **82,** 1604–1608.
37. Chothia, C. (1984) *Annu. Rev. Biochem.* **53,** 537–572.
38. Bjorkman, P. J., Saper, M. A., Samraoui, B., Bennett, W. S., Strominger, J. L. & Wiley, D. C. (1987) *Nature (London)* **329,** 506–512.
39. Sprang, S. R., Fletterick, R. J., Goldsmith, E. J., Madsen, N. B., Acharaya, K. R., Stuart, D. J., Varvill, K. & Johnson, L. N. (1988) *Nature (London)* **336,** 215–221.